

The circumbinary disk of HD 98800 B: Evidence for disk warping

R. L. Akeson¹, W.K.M. Rice², A.F. Boden¹, A.I. Sargent³, J.M. Carpenter³, G. Bryden⁴

ABSTRACT

The quadruple young stellar system HD 98800 consists of two spectroscopic binary pairs with a circumbinary disk around the B component. Recent work by Boden and collaborators using infrared interferometry and radial velocity data resulted in a determination of the physical orbit for HD 98800 B. We use the resulting inclination of the binary and the measured extinction toward the B component stars to constrain the distribution of circumbinary material. Although a standard optically and geometrically thick disk model can reproduce the spectral energy distribution, it can not account for the observed extinction if the binary and the disk are co-planar. We next constructed a dynamical model to investigate the influence of the A component, which is not in the Ba-Bb orbital plane, on the B disk. We find that these interactions have a substantial impact on the inclination of the B circumbinary disk with respect to the Ba-Bb orbital plane. The resulting warp would be sufficient to place material into the line of sight and the non-coplanar disk orientation may also cause the upper layers of the disk to intersect the line of sight if the disk is geometrically thick. These simulations also support that the dynamics of the Ba-Bb orbit clear the inner region to a radius of ~ 3 AU. We then discuss whether the somewhat unusual properties of the HD 98800 B disk are consistent with material remnant from the star formation process or with more recent creation by collisions from larger bodies.

Subject headings: binaries: spectroscopic — circumstellar material — stars:formation — stars: individual(HD 98800B)

¹Michelson Science Center, California Institute of Technology, Pasadena, CA, 91125

²Scottish Universities Physics Alliance (SUPA), Institute for Astronomy, University of Edinburgh, Blackford Hill, Edinburgh, EH9 3HJ, Scotland

³Dept. of Astronomy, California Institute of Technology, Pasadena CA 91125

⁴Jet Propulsion Laboratory, California Institute of Technology, Pasadena, CA, 91108

1. Introduction

As the majority of stars are formed in binary or higher order multiple systems, understanding the effects of multiplicity is essential to understanding star formation. HD 98800 is a member of the TW Hydra association, whose members have distances from 40 to 100 pc (*Hipparcos*; Perryman et al. 1997), and is a quadruple system comprising two spectroscopic binaries (Torres et al. 1995), HD 98800 A and B, both with K star primaries. The AB pair has a separation of $0''.8$, corresponding to 34 AU and a period of 300-430 years (Tokovinin 1999). Age estimates for the TW Hya association range from 5 to 20 Myr (Soderblom et al 1998, and references therein) and several members including HD 98800 (Zuckerman & Becklin 1993), have significant infrared excess emission.

Gehrz et al. (1999), Koerner et al. (2000) and Prato et al (2001) resolved the AB system excess and determined that the mid-infrared excess arises from material around the B spectroscopic binary, the northern component. The excess is detected only at wavelengths longer than 8 microns and is well fit by a 150 K blackbody (Low et al. 1999; Koerner et al. 2000; Prato et al 2001). Recent *Spitzer* IRS observations by Furlan et al (2007) show a small excess starting at $5.5 \mu\text{m}$ with the majority of the excess at wavelengths of $8 \mu\text{m}$ and longer. At this temperature the material is several AU from the stars and must therefore be circumbinary given the semi-major axis of 0.98 AU (Boden et al. 2005). HD 98800 shows no sign of active accretion as judged by the $\text{H}\alpha$ line width of 0.19 Angstroms (Dunkin et al. 1997) or X-ray emission (Kastner et al. 2004). This is in contrast with two of the other association members, TW Hya and Hen 3-600 A, which have observed accretion rates only 1-2 orders of magnitude lower than those in 1 Myr-old T Tauri stars (Muzerolle et al. 2000).

Circumbinary disks are not uncommon around closely spaced (separation less than a few AU) young stellar binaries (Jensen & Mathieu 1997). However, at an age of 10 Myr, 80-90% of young stars have dispersed their primordial disk as traced by near and mid-infrared excess (Hillenbrand 2007). The population of main sequence stars with an infrared excess (the so-called debris or secondary disk systems) discovered by IRAS (Aumann et al. 1984) has been greatly expanded by the sensitivity of *Spitzer*. Recent *Spitzer* observations show $\sim 15\%$ of A to K spectral type field dwarfs have a mid-infrared excess (e.g. Beichman et al. (2006); Chen et al. (2006)), but the material in these disks is believed to arise from collisions between larger bodies rather than being primordial and many of these stars have an excess only at wavelengths $> 20 \mu\text{m}$, indicative of cool dust.

Determining the evolutionary state of the HD 98800 B circumbinary disk is complicated by multiplicity. Secondary disks are also observed around main sequence binaries (Trilling et al. 2007) as they are around pre-main sequence binaries (Jensen & Mathieu 1997). Dynamical studies have shown that a circumbinary disk will have a cleared cen-

tral region which can greatly slow or stop material from accreting onto the central star (Artymowicz & Lubow 1994; Pichardo et al 2005). Thus it is not clear if the material surrounding B is remnant from the star formation process or has been created by collisions from larger bodies.

Recently, Boden et al. (2005) used measurements from the Keck Interferometer, the *Hubble Space Telescope* Fine Guidance Sensors and radial velocity data to determine the physical orbit of HD 98800 B and the mass and luminosity of its components. Boden et al. (2005) modeled the SEDs of the HD 98800 B components, finding effective temperatures of 4200 ± 150 K and 4000 ± 150 K, and luminosities of $0.330 \pm 0.017 L_{\odot}$ and $0.167 \pm 0.038 L_{\odot}$ for the primary and secondary respectively. Additionally, a small extinction of $A_V 0.3 \pm 0.05$ was required to fit the SED of the system. Soderblom et al (1998) also found that a small extinction ($A_V \approx 0.44$ mag) was necessary to explain the lithium-predicted visible photometry. Soderblom et al (1998) additionally noted the significant time variability with no obvious periodicity in the *Hipparcos* optical photometry, which Tokovinin (1999) suggests may be due to extinction through an edge-on disk. In contrast, an earlier monitoring campaign by Henry & Hall (1994) detected a 0.07 magnitude variation at V with a 14 day period which they suggest is due to a starspot; however, these authors were unaware of the dual spectroscopic binary composition of the HD 98800 system.

In this paper, we use the orbital parameters and the observed SED to constrain the physical properties of the circumstellar material around HD 98800 B. In §3, we investigate the origin of the extinction towards HD 98800 B given the inclination of the binary orbit using geometrically thick circumstellar disk models. In §4, we present a dynamical simulation of the interaction between the A and B components and the B disk. In §5, we compare our results to other models of the HD 98800 B disk and discuss the implications of the modeling on the question of whether the disk material is primordial or secondary and on the origin of the extinction along the line of sight to HD 98800 B. Our conclusions are summarized in §6.

2. Input data

2.1. Photometry

We use near-infrared through sub-millimeter photometry from the literature (Prato et al 2001; Sylvester et al. 1996) to determine the flux contribution of the disk. In this work, we concentrate only on the continuum emission and do not use the photometry affected by the $10 \mu\text{m}$ silicate feature. Koerner et al. (2000) and Prato et al (2001) discuss this spectral feature and recent work by Furlan et al (2007) using the *Spitzer* mid-infrared spectrum sug-

gests the presence of amorphous carbon, pyroxene and olivine grains. The stellar effective temperatures, luminosities and system distance are taken from Boden et al. (2005).

2.2. Orbital parameters

We use the relevant orbital parameters from Boden et al. (2005) (Table 1) to derive the dynamical constraints on the disk. Circumstellar material will tend to be cleared from the inner disk region through interactions with the central stars (see e.g. Artymowicz & Lubow 1994; Pichardo et al 2005) and this clearing increases with the orbital eccentricity of the binary. For HD 98800 B the apastron distance is 1.75 AU, making any material within this radius dynamically unstable. From the calculations of Pichardo et al (2005) the circumbinary disk for a system such as HD 98800 B with eccentricity of 0.78 and secondary mass fraction $m_2/(m_1 + m_2) = 0.45$ is cleared to a radius of 3.5 times the semi-major axis or 3.4 AU.

e	0.7849 ± 0.0053	
i (deg)	66.8 ± 3.2	
a (mas)	23.3 ± 2.5	
System distance (pc)	42.2 ± 4.7	
	Ba	Bb
Mass (M_\odot)	0.699 ± 0.064	0.582 ± 0.051
T_{eff} (K)	4200 ± 150	4000 ± 150
Luminosity (L_\odot)	0.330 ± 0.075	0.167 ± 0.038

Table 1: Orbital and physical parameters for HD 98800 B from Boden et al. (2005).

The outer radius was derived using similar constraints from the A-B orbit parameters from Tokovinin (1999; a = 62 AU and e = 0.5; Orbit II), an A component total mass of 1.3 M_\odot and the circumsecondary truncation results shown in Figure 7 of Artymowicz & Lubow (1994) for a viscosity of 10^{-3} . Although the Artymowicz & Lubow (1994) models are for a circumsecondary disk in a planar orbit and the A-B and Ba-Bb orbits are not coplanar (Tokovinin 1999) we use this as a guide to how any material distributed around B would be dynamically influenced by the A-B orbit and these inner and outer truncation radii are confirmed for the case of HD 98800 B by the dynamical model presented in §4.

2.3. Extinction

Mid-infrared imaging from Koerner et al. (2000) and Prato et al (2001) indicated the large IR excess in HD 98800 is associated with HD 98800 B, with no significant excess emission from HD 98800 A. Spectroscopic and interferometric observations that resolve the flux ratios from the B subsystem components allowed Boden et al. (2005) to model the B subsystem SED, and assess the individual component temperatures and luminosities. The Boden et al. (2005) SED modeling required a small amount of extinction to match visible HST photometry; a similar conclusion was drawn by Soderblom et al (1998) using visible spectroscopy. Finally, both groups concluded that no extinction is apparent in the SED of HD 98800 A. The association of IR excess and extinction with B and not A suggests that there is circumbinary material around the B subsystem.

To quantify the column density of dust which would produce $A_V 0.3 \pm 0.05$, we used the dust parameters of Wood et al. (2002) derived for the HH 30 disk. These parameters are most likely to be appropriate if the extinction arises due to the line of sight passing through some portion of the HD 98800 B circumbinary disk and assuming a similar composition for the HH 30 and HD 98800 B disks. At V ($0.55 \mu\text{m}$), the dust mass opacity from Wood et al. (2002) is $35 \text{ cm}^2/\text{gm}$. For an extinction of $A_V 0.3 \pm 0.05$, this results in a column density of $8 \times 10^{-3} \text{ g/cm}^2$. For comparison, the surface density of the minimum mass solar nebula at 1 AU is $\sim 10^3 \text{ g/cm}^2$ (Weidenschilling 1977), thus if the extinction is due to the line of sight passing through the disk, it is only through the tenuous outer layers.

3. Circumbinary disk models

Several previous groups have successfully reproduced the SED of HD 98800 B with a $\sim 150 \text{ K}$ blackbody (Low et al. 1999; Koerner et al. 2000; Prato et al 2001; Furlan et al 2007). However, none of these groups included all the dynamical constraints ($3 \lesssim R_{stable} \lesssim 10 \text{ AU}$) and the unresolved mid-IR imaging of Prato et al (2001). Here we consider if a geometrically thick dust and gas disk can reproduce the SED while fitting both the dynamical constraints and intersecting the line of sight to provide the observed extinction.

We use a Bayesian approach to characterize the disk parameters; this approach has been used to characterize disks around young stars by Lay et al. (1997) and Akeson et al. (2002). We fix some of the physical characteristics based on the assumption of the circumbinary disk being co-planar with the B binary orbit (i.e. inclination) and other parameters based on the physics of the input model (i.e. radial temperature gradient). For the remaining parameters we use the Bayesian formalism to calculate a probability distribution for each parameter.

This method shows how well a given parameter is constrained and how the free parameters may be degenerate with each other, which is a particular concern using only spatially unresolved data. It also facilitates the inclusion of additional observational constraints (e.g. the dynamical truncation radii). In our case, the assumptions made (the inclination angle and co-planarity of the disk and the Ba-Bb orbit) do not have associated probabilities, so the relative likelihood a single model, given the known data set, is proportional to $e^{-\chi^2/2}$. This probability is calculated for every possible set of parameter values. Then, for each parameter value, the relative probability is the sum of all probabilities for the range of values in all the other parameters.

3.1. Flared accretion disk

We first consider a disk with physical properties relevant to the active accretion phase of younger T Tauri stars and in particular, consider a flared disk model to investigate if the extinction can arise from the line-of-sight intersecting the outer regions of a flared disk. A simple calculation shows that this is plausible. The exact form of the disk height (H) as a function of radius (r) depends on the disk temperature profile and ranges from $H \propto r^{9/8}$ to $H \propto r^{9/7}$ (Kenyon & Hartmann 1987; Chiang & Goldreich 1997). Here, we use the relations derived by Chiang & Goldreich (1997) where at radii relevant to the HD 98800 B disk $H = 0.17r^{9/7}$ where r is the disk radius in AU. Therefore the angle of incidence (α) for light from the central star is $\tan \alpha = H/r = 0.17r^{2/7}$. From Boden et al. (2005), the orbital inclination angle is $67^\circ \pm 3^\circ$ and therefore $\alpha > 23^\circ$ when $r > 25$ AU (Figure 1). Although an outer radius this large is probably ruled out by the A-B orbit truncation effects, the observed column is so small that it may arise from material above the disk scale height.

To further investigate the possibility that the extinction arises from the outer regions of a flared disk we parameterized the Chiang & Goldreich (1997) disk and determined the disk properties as constrained by the SED data. The disk is comprised of an interior and a superheated surface. For the wavelengths and radii under consideration in the HD 98800 B disk, the surface layer is always optically thin and so the surface flux is simply added to the interior flux (which may be optically thick). To account for a different stellar flux than in the original model, we use the interior T_i and surface T_s temperature radial scalings from Chiang & Goldreich (1997), but include an single scaling factor T_o ,

$$T_i = T_o(150/r^{3/7}) \text{ K} \tag{1}$$

$$T_s = T_o(550/r^{2/5}) \text{ K}, \tag{2}$$

where r is the radial distance in AU. The surface density (Σ) and its radial exponent (p) are also allowed to vary. The resulting model has six parameters: T_o, Σ_o (surface density at 2

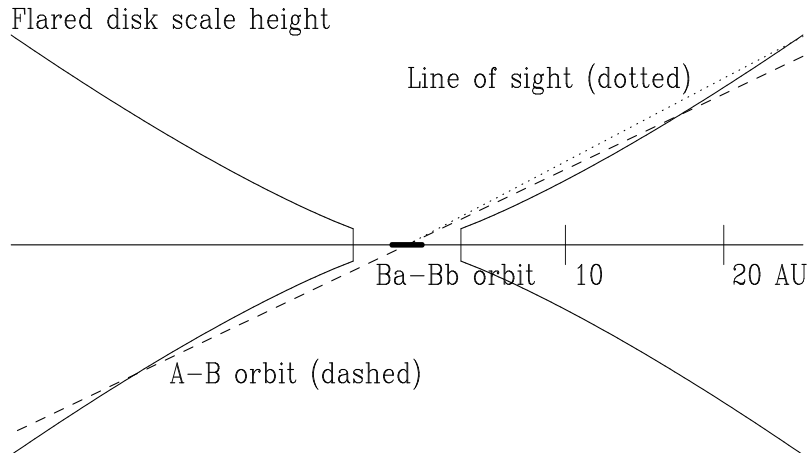


Fig. 1.— Illustration of the angles and scales for the HD 98800B system. The figure is looking edge-on to the Ba-Bb orbit (thick solid line) with the center of mass at the origin. The inferred line-of-sight to Earth is shown as a dotted line and the angle with the A-B orbit is shown as a dashed line. The scale height for a flared disk following the Chiang & Goldreich (1997) calculations (§3.1) is also shown, with an inner radius of 3.4 AU. The outer radius is deliberately unconstrained to demonstrate where the disk would intersect the line-of-sight if the radial extent were sufficiently large.

AU), p , r_{in} , Δr (disk radial extent) and β (dust opacity frequency exponent) and the range of values searched for each is given in Table 2. The inclination angle is set at 67° .

All parameters have a range of values which are contained within models which roughly match the SED. Table 2 gives the 90% probability range for each parameter. We note that these models tend to produce too much flux in the mid-infrared, which can be eliminated by removing the surface layer and having a single layer disk; however, the probability distribution for the inner radius for the single layer models does not include any models where $r_{in} > 3$ AU (fitting the dynamical constraints). It may be possible to produce a better fit to the mid-infrared SED and satisfy the dynamical constraints with modifications to the temperature structure of the disk, but we did not wish to add more parameters. In comparison to the single temperature fits (Low et al. 1999; Prato et al 2001) the interior temperatures at the inner radius are below 150 K, but this is balanced by the much hotter surface layer. An example model, along with the SED data used for the stellar photosphere fit (Boden et al.

Parameter	Range searched	90% prob. range
T_o	0.35 – 0.7	0.45 – 0.6
Σ (gm/cm ²)	0.02 – 3	0.025 – 0.5
p	0.5 – 2.5	unconstrained
Δr (AU)	0.2 – 4	0.8 – 2.0
r_{in} (AU)	1 – 4	1.1 – 3.6
β	0 – 2	0.15 – 0.9

Table 2: Range of values searched for each parameter of the flared disk model and the range of values which encompasses a probability range of 90%.

(2005)) and the data used in the disk modeling, are shown in Figure 2. The SED can be roughly reproduced with a range of inner radii from 1.1 to 3.6 AU. Interestingly, all the probable models have a relatively small radial extent ($\Delta r < 2$ AU) with the 90% probability range from 0.8 to 2.0 AU. A disk with this extent would appear unresolved in the mid-infrared imaging (consistent with Koerner et al. 2000; Prato et al 2001).

We can now calculate if the models which reproduce the SED can also explain the observed extinction. Using an example model with $r_{in} = 3.2$ AU, $\Delta r = 0.8$ AU and a surface density of 0.035 gm/cm² at a radial distance of 2 AU, the column density along the derived line of sight is $\sim 10^{-12}$ gm/cm², with similar column densities derived for other models with high relative probabilities. For the Chiang & Goldreich (1997) model visible dust opacity of $\kappa_V \sim 400$ cm²/gm, this results in an extinction of $A_V \sim 10^{-11}$, many orders of magnitude below the observed extinction of 0.3 ± 0.05 .

3.2. Vertically extended inner radius

Next, we considered if the extinction could arise from a vertically extended rim at the inner disk radius. Vertically-extended inner rims arise from direct irradiation of dust (Natta et al. 2001; Dullemond et al. 2001) at the inner disk edge. From Dullemond et al. (2001) the pressure scale height is

$$h_{rim} = \frac{kT_{rim}R_{rim}^3}{\mu_g GM_\star}^{1/2} \quad (3)$$

where h_{rim} , T_{rim} and R_{rim} are the pressure scale height, temperature and radius of the inner rim, μ_g is the mean molecular weight of the gas and the rim height $H_{rim} \approx 5h_{rim}$. Using a

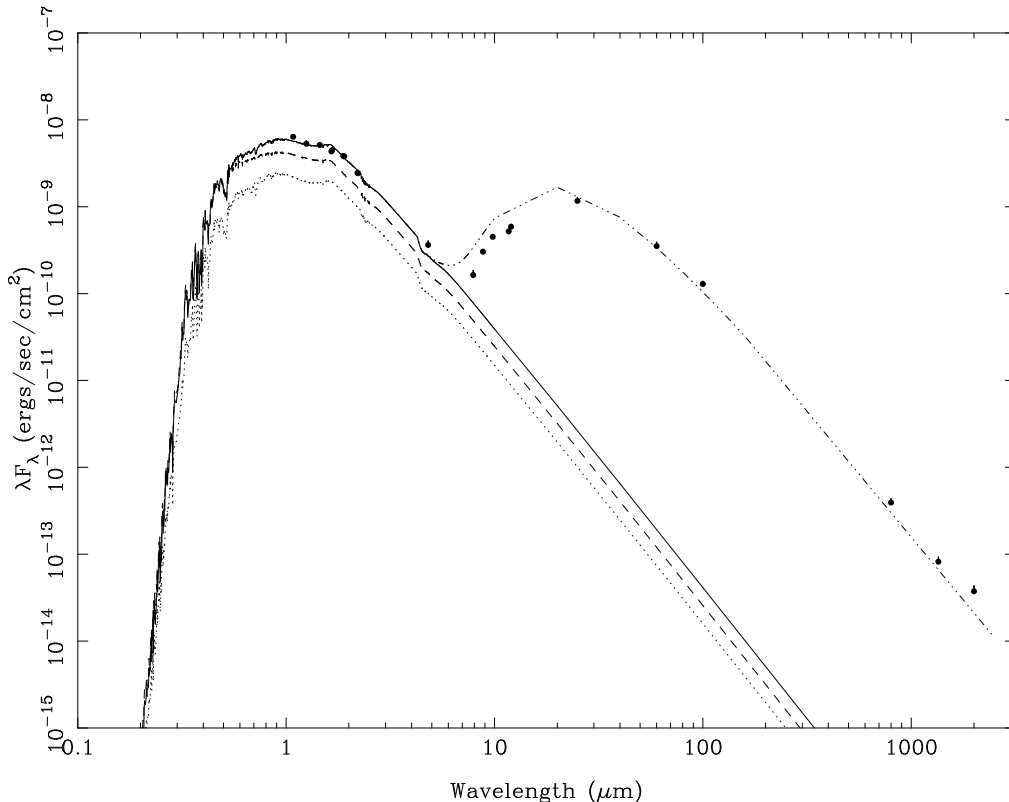


Fig. 2.— The stellar photosphere models for the components of HD 98800 B (dashed = Ba, dotted = Bb, solid=total) along with photometry from the literature. The optical to near-infrared photometry was used for the stellar fit, while the mid-infrared to millimeter photometry was used for the disk modeling. The photometry is taken from Prato et al (2001) and Sylvester et al. (1996) and where error bars are not visible, they are smaller than the symbol size. An example flared disk model (dot-dashed) is shown with $T_o=0.61$, $\Sigma = 0.035$ gm/cm², $p = 1$, $r_{in} = 3.1$ AU, $\Delta r = 0.8$ AU and $\beta = 0.8$.

combined mass of $1.28 M_{\odot}$, $\mu_g = 2$ and $T_{rim}=150$ K,

$$H_{rim} \approx 0.12 \left(\frac{R_{rim}}{AU} \right)^{1/2} AU. \quad (4)$$

If the inner disk is dynamically truncated by the binary orbit at a radius of 3.4 AU (§2.2), the height of the rim is 0.41 AU. A rim at this radius and height would obscure the line of sight starting at an inclination angle of 85°. Given the inclination angle of the binary orbit

of $67^\circ \pm 3^\circ$, the inner disk rim will not obscure the line-of-sight if the disk is co-planar with the binary orbit.

3.3. Circumbinary envelope

Finally, we consider the possibility that the extinction towards HD 98800 B could arise from material distributed in a circumbinary envelope around the B pair. Assuming a spherical distribution, the surface density calculated above can be used to estimate the total mass in such an envelope if the inner and outer radius are known. For the purpose of a rough mass estimate, we use a value for the inner radius from the region cleared by the B orbit of 3.4 AU and a value for the outer radius of 10 AU (§2.2), which results in an envelope mass of $5 \times 10^{-7} M_\odot$.

Circumstellar envelopes are common around young stars with ages of a few Myr but have generally dissipated at the derived age of HD 98800 B (e.g., Mundy, Looney, & Welch 2000). However, the dynamics of the quadruple system are significantly more complicated than considered in the canonical star formation picture and a small amount of material from the formation of the central stars may have been unable to accrete onto the disk. We consider this unlikely given that the A component, which has a similar mass and is presumably coeval has no such material.

4. Dynamical simulations

The HD 98800 B circumbinary disk exists within the dynamical environment of the larger quadruple system and could be warped by interactions with HD 98800 A. To model the HD 98800 dynamical environment, we consider a system comprising 3 stars. Two of these stars represent the HD 98800 B system with masses of $M_1 = 0.699M_\odot$ and $M_2 = 0.582M_\odot$, an orbital period of 315 days and an eccentricity of $e = 0.78$. These two stars are then surrounded by a circumbinary disk comprising 25000 test particles with an initial inner radius of 2 AU and an outer radius of 15 AU. The disk particles were distributed randomly with no initial eccentricity, but with initial inclinations that were Rayleigh-distributed, with the sine of the inclinations, $\sin i$, having a root mean square value of 0.05. The disk is therefore initially thin, but not completely flat.

The HD 98800 A binary system was then represented by a single star with a mass equal to the combined mass of the two stars representing the HD 98800 B system ($M_3 = 1.281M_\odot$). Although we could have modeled HD 98800 A using two stars, the actual orbital parameters

and stellar masses are not well known, and this would have been computationally expensive. Representing HD 98800 A with a single star is an approximation that should at least give us some idea of how this outer system influences the disk around HD 98800 B. The orbital period of the A-B system was taken to be 345 years with an eccentricity of $e = 0.5$ (Tokovinin 1999, Orbit II) and with an orbital plane initially inclined at 10° to the plane of the disk around HD 98800 B, which is coincident with HD 98800 B’s orbital plane.

In this dynamical simulation we have ignored radiation pressure and Poynting-Robertson drag (Burns et al. 1979). HD 98800 is a young system and the disk around HD 98800 B is relatively massive and is collisionally dominated (Wyatt et al. 2006). Poynting-Robertson drag in a system like HD 98800 B is therefore expected to be insignificant because dust will be destroyed by collisions before Poynting-Robertson drag can cause significant inward migration (Wyatt 2005). Although radiation pressure could change the orbital parameters of particles produced by collisions (Wyatt et al. 1999), the pericenters of these orbits should be randomly orientated and so the effect will be to spread these particles out without changing the plane of their orbits. Since this is unlikely to affect significantly the global structure of the disk we ignore it here and include only the gravitational influence of the stars.

The system was evolved for just over 10^6 years using a Hermite integrator (Makino 1991), that conserved both energy and angular momentum to within 0.1%. We found that the star representing HD 98800 A caused the HD 98800 B binary system and its circumstellar disk to undergo torque induced precession with a period of ~ 99000 years. The inclination of the HD 98800 B system, with respect to the initial plane of the HD 98800 A/B orbit, also varies sinusoidally from the initial 10° to just over 20° with a period of ~ 43000 years.

Figure 3 shows the variation of the disk structure over one precession period from $t = 1.0823$ Myr to $t = 1.1841$ Myr. In each panel the center of mass of the HD 98800 B system is located at the origin, and each panel shows a thin slice through the circumbinary disk together with the central stars of the HD 98800 B system. In these figures, the x-y plane is the initial plane of the orbit of the HD 98800 A/B system. The orbital plane of HD 98800 B and its circumbinary disk were therefore initially inclined at 10° to the x-y plane. The label on each figure shows the time, the viewing angle (ϕ), and the inclination of the orbital plane of HD 98800 B relative to the x-y plane (θ). The viewing angle is varied to take into account the precession of HD 98800 B, such that the disk is always viewed along the axis, in the x-y plane, about which the disk appears to have been rotated.

What the panels in Figure 3 show is that the eccentric orbit of HD 98800 B ($e = 0.781$) truncates the inner disk at a radius of ~ 3 AU (in agreement with the estimates in §2.2), while the outer disk, which initially extended to a radius of 15 AU, is now truncated at a radius of ~ 10 AU due to the influence of HD 98800 A. Note that this outer truncation radius

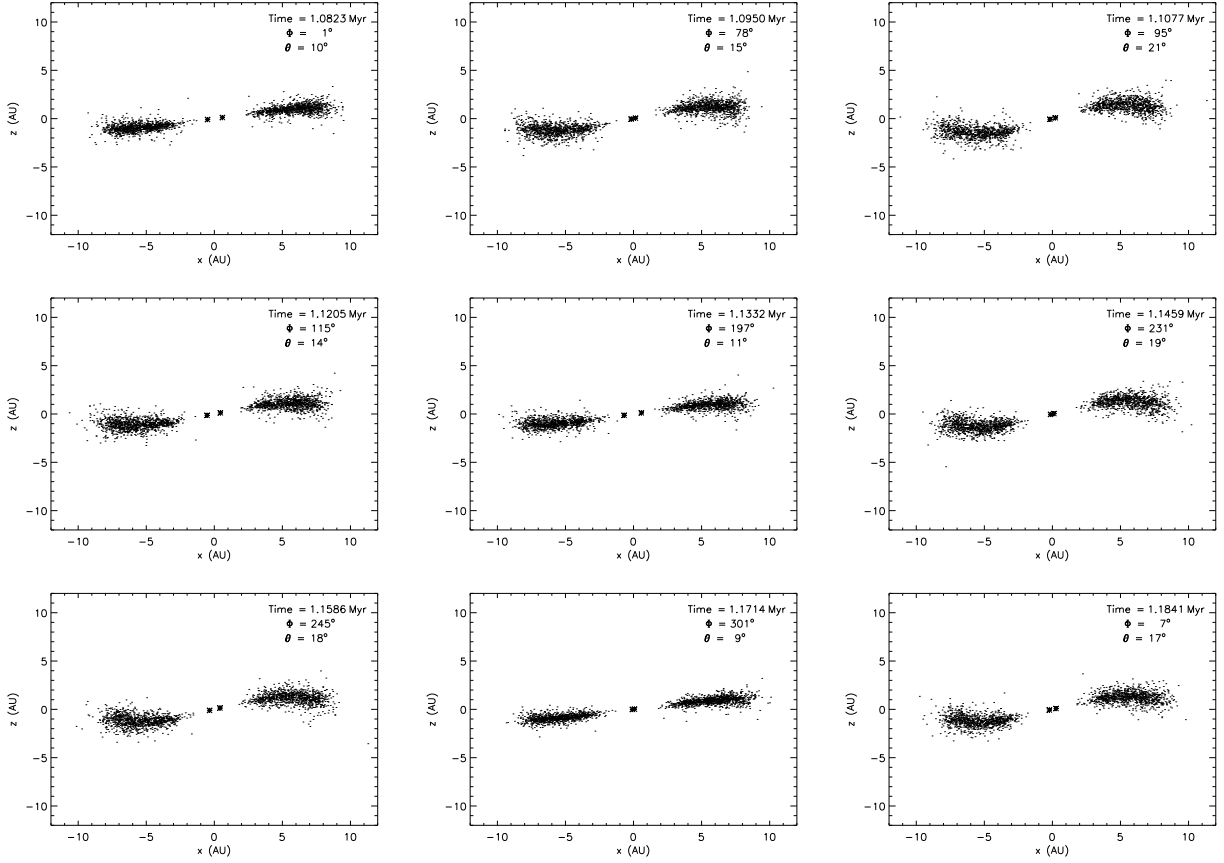


Fig. 3.— A series of figures showing the evolution of the circumbinary disk around HD 98800 B over one precession period. The center of mass of HD 98800 B is located at the origin and the x-y plane is the initial plane of the HD 98800 A/B orbit. Each panel shows a slice through the circumbinary disk together with the two central stars. The viewing angle (ϕ) is varied to take into account the precession of the system and such that the disk is always viewed along the axis, the in x-y plane, about which the disk appears to have been rotated. Not only do these figures illustrate how the inner and outer disk are truncated, they also illustrate how the disk becomes warped as the angle, θ , between the orbital plane and the x-y axis increases. This warping is qualitatively consistent with the visual extinction observed towards HD 98800 B, which has an inclination angle of 67° .

also agrees with the estimates based on co-planar interactions (§2.2). This outer radius value further supports the idea that the observed visual extinction to HD 98800 B is unlikely to be due to a flared co-planar disk extending to large radii. What is also clear from Figure 3 is that when the inclination of the orbital plane relative to x-y plane is small ($\theta \sim 10^\circ$), the disk is thin and slightly flared. However, as the angle increases, the disk becomes more

obviously warped. Consider the third panel in the top row. The orbital plane is inclined at 21° to the x-y axis and yet a line of sight along the x-axis would still intercept some disk material.

Although the resolution of our simulation is insufficient to quantify the column density of material located more than 20° above the orbital plane of HD 98800 B, the existence of the warp is qualitatively consistent with the observed extinction to HD 98800 B, the orbit of which has an inclination angle of 67° , particularly given the low column density required to produce the observed extinction. This is consistent with the observed variability in the Hipparcos data (Soderblom et al 1998) arising from changes in extinction if the disk material is clumpy, but as these simulations can not quantify the column density, we can not directly compare to the variability. The rotation time scale of the warp is much longer than the 14 day periodic variations observed by Henry & Hall (1994) which does not correspond well to the disk rotation time scale of 2.5 yrs at 3 AU.

5. Discussion

In this section, we first compare our results on the circumbinary disk of HD 98800 B to models of this disk from other authors. Next we compare the HD 98800 B disk to samples of other objects with primordial and secondary disks, discuss the implications for the evolutionary status of this object and suggest some observational tests of this status.

5.1. Comparison to other models

As listed in §1 and §3, several other groups have modeled the disk of HD 98800 B (Low et al. 1999; Koerner et al. 2000; Prato et al 2001; Furlan et al 2007). All these models have the following characteristics in common: a circumbinary disk with a inner region cleared to at least a few AU dominated by emission from material with a temperature of ~ 150 K. Here we compare to the Prato et al (2001) and Furlan et al (2007) models which use either imaging constraints or detailed spectroscopy in their modeling. Using their unresolved images as constraints, Prato et al (2001) fit the SED with a blackbody temperature of 150 K and derived an inner radius 2 AU, an outer radius of at least 5 AU, and a possible cooler dust component at larger radii which is then truncated by the A/B component interactions. They also comment that the vertical extent must be ~ 1.5 AU to account for the high fractional luminosity. Our dynamical simulations and the work of Artymowicz & Lubow (1994) and Pichardo et al (2005) suggest that this inner radius is too small to be stable given the orbital

parameters of the binary.

Recently, Furlan et al (2007) used the mid-infrared spectrum of HD 98800 from the Spitzer telescope to constrain the structure and composition of the HD 98800 B disk. Their spectrum shows no excess below $5.5 \mu\text{m}$ (within a 5% absolute calibration) and a strong excess starting at $8 \mu\text{m}$. They use the structure in the silicate feature to model the dust composition and we refer interested readers to the paper for more details on that aspect. In comparison to our model, the relevant model parameters are an optically thick region starting at 5.9 AU with a temperature of 150 K and an optically thin ring between 1.5 and 2 AU with grain sizes of a few microns and a temperature of 310 K where the silicate emission features arise from. This inner ring is within the apastron separation of the Ba-Bb pair of 1.75 AU and within the dynamically cleared regions in the work of Artymowicz & Lubow (1994), Pichardo et al (2005) and §4. If material is located at these radii, it will be transient as the time scales for clearing the gap (<100 orbital periods, i.e. <100 yrs) are much shorter than the P-R drag timescale of 10^5 yrs for a $3 \mu\text{m}$ grain at 3 AU in this system. HD 98800 B also shows no indication of accretion, unlike the DQ Tau and UZ Tau E systems which are inferred to have active accretion through streamers from a circumbinary disk (Mathieu et al. 1997; Jensen et al. 2007).

Both Prato et al (2001) and Furlan et al (2007) noted that small grains must be present in the HD 98800 B disk to account for the spectral features. A distribution of grains size is inferred in many pre-main sequence, primordial disks (see review by Natta et al. 2007) and the higher temperatures silicate grains inferred by Furlan et al (2007) from features in the mid-infrared spectrum could reside on the stellar photon-illuminated surface of a flared or warped disk such as that discussed in §3.1. In the example model presented in Figure 2, the interior temperature at the inner rim is 60 K, while the surface layer temperature is 210 K. Spectrally resolved mid-infrared interferometry observations would constrain the location of the small grains responsible for the silicate emission feature.

5.2. Comparison to other primordial and secondary disks

The TW Hya association is unusual in containing sources with a very large range of pre-main sequence properties. Four of the sources have *IRAS*-detected infrared excesses (TW Hya, HD 98800, Hen 3-600 and HR 4796A). TW Hya and Hen 3-600 are often classified as T Tauri stars given their accretion signatures (Muzerolle et al. 2000) and near-infrared excess, and TW Hya has observed CO and H₂ in the disk (Dent et al. 2005; Weintraub et al. 2000). On the other hand, HR 4796A has a similar SED to HD 98800, but with material at much larger radii and is consistent with a secondary dust debris disk. Thus, it is not

clear from the association as a whole whether the HD 98800 B disk is primordial or secondary. Here we compare the derived disk properties of HD 98800 B with those of other primordial/protostellar and secondary/debris disk systems.

The mass distribution of the most probable models from §3.1 for a flared gas and dust disk peaks at $10^{-7} M_{\odot}$, significantly lower than most classical T Tauri stars and comparable to many secondary debris disk stars such as the beta Pic moving group (e.g. Meyer et al. (2007)); however, as shown in §4, the HD 98800 B circumbinary disk is likely to be dynamically truncated at both the inner and outer radii, and the disk mass is highly correlated with the small radial extent (few AU) as compared to values of ~ 100 AU typical for T Tauri circumstellar disks. An additional contribution to the low disk mass is the surface density of $< 0.5 \text{ gm/cm}^2$ at a radius of 2 AU, which is a factor of ~ 100 lower than the minimum mass solar nebula. The high infrared luminosity of the disk ($0.1 - 0.2 L_{*}$) has been noted by many groups (Zuckerman & Becklin 1993; Koerner et al. 2000; Prato et al 2001) and this fraction is significantly higher other young debris disks systems, such as the sample observed by Chen et al. (2006) of A to M spectral types with ages < 50 Myr. In that sample, the detected systems had infrared disk luminosities of $5 \times 10^{-6} - 5 \times 10^{-3} L_{IR}/L_{*}$. However, the dust in those systems is in general located many to tens of AU from the central star, rather than a few AU and is not likely to be as vertically extended. Overall, the disk properties for HD 98800 B are intermediate between those of T Tauri, primordial disks (and its association members TW Hya and Hen 3-600) and secondary debris disks around stars with ages of tens of Myr.

A more stringent diagnostic of primordial vs. secondary material would be to observe gas tracers in the disk and establish the gas to dust ratio. In a CO survey by Dent et al. (2005), HD 98800 was not detected with an upper limit of 0.09 K km/sec, while TW Hya was detected with 2.16 K km/sec of emission. Although their relative infrared excesses (~ 0.1 for HD 98800 and 0.3 for TW Hya) are similar, the difference in CO emission strengths may result primarily from the CO arising in colder gas 10's of AU from the star. As the HD 98800 B disk is probably much smaller than this, the CO non-detection does not set stringent limits on gas depletion.

The lack of accretion signature in HD 98800 B is not surprising in the context of a ~ 3 AU inner hole; however, accretion across the gap in a circumbinary disk can take place (Artymowicz & Lubow 1996), particularly for geometrically thick disks and has been observed in T Tauri circumbinary disks such as DQ Tau and UZ Tau E (Mathieu et al. 1997; Jensen et al. 2007). Dynamical modeling by Artymowicz & Lubow (1996) shows that the mass accretion from circumbinary disks is strongly modulated in time and peaks at periastron. Thus another observational test for the HD 98800 B disk would be time monitoring of

accretion diagnostics, particularly centered about periastron.

6. Summary

HD 98800 B is one of the few young multiple stars with significant disk emission for which the physical orbit has been determined. We have used the orbital parameters, particularly the inclination, and the assumption of disk-binary coplanarity to examine physical models for the disk. As first discussed by Prato et al (2001) the large mid-infrared excess and unresolved images of HD 98800 B seem to require an optically and geometrically thick disk. Either a flared disk or a vertically extended inner rim can satisfy the geometric requirement, but dynamical truncation will keep the majority of the material beyond an inner rim with a radius of 3 AU. The disk solution presented here is not unique in reproducing the SED and somewhat over-produces mid-infrared continuum flux, but does satisfy the dynamical constraints.

We find that a standard disk prescription is unable to explain the observed extinction if the disk and the binary orbit are co-planar. For the flared disk model in Figure 2 to intercept enough of the line of sight to produce the observed extinction, the disk inclination would need to be 81° as compared to the binary orbit inclination of 67° . From the dynamical simulations shown in §4, interactions between the B circumbinary disk and the A component are sufficient to perturb the disk inclination by that amount. They are also sufficient to warp a thin disk enough to place material into the observed line of sight. In either case, we suggest that the small observed extinction is due to significant perturbations of the circumbinary disk by the A binary component in this quadruple system. The next step in understanding the HD 98800 B disk would be to quantitatively combine the SED and observational imaging constraints (unresolved mid-infrared size and extinction along the line of sight) with the dynamical interactions between all the components in the HD 98800 system.

We thank Sverre Aarseth for help with the use of his N-body codes and Kenneth Wood for initial SED modeling. We also thank Peter Brand and Mark Wyatt for useful discussions about secular perturbation theory. We are grateful to the anonymous referee for several helpful suggestions.

REFERENCES

- Akeson, R. L., Ciardi, D. R., van Belle, G. T., & Creech-Eakman, M. J. 2002, *ApJ*, 566, 1124
- Artymowicz, P. and Lubow, S. 1994 *ApJ* 421, 651.
- Artymowicz, P., & Lubow, S. H. 1996, *ApJ*, 467, L77
- Aumann, H. H., et al. 1984, *ApJ*, 278, L23
- Backman, D. E., Witteborn, F. C., & Gillett, F. C. 1992, *ApJ*, 385, 670
- Beichman, C. A., et al. 2006, *ApJ*, 652, 1674
- Boden, A. F., et al. 2005, *ApJ*, 635, 442
- Burns, J. A., Lamy, P. L., & Soter, S. 1979, *Icarus*, 40, 1
- Chen, C. H., et al. 2006, *ApJS*, 166, 351
- Chiang, E. I., & Goldreich, P. 1997, *ApJ*, 490, 368
- Dent, W. R. F., Greaves, J. S., & Coulson, I. M. 2005, *MNRAS*, 359, 663
- Dullemond, C. P., Dominik, C., & Natta, A. 2001, *ApJ*, 560, 957
- Dunkin, S. K., Barlow, M. J., & Ryan, S. G. 1997, *MNRAS*, 290, 165
- Furlan, E., 2007, *ApJ*, in press
- Gehrz, R. D., Smith, N., Low, F. J., Krautter, J., Nollenberg, J. G., & Jones, T. J. 1999, *ApJ*, 512, L55
- Henry, G. W., & Hall, D. S. 1994, *ApJ*, 425, L25
- Hillenbrand, L.A., 2007, *A Decade of Discovery: Planets Around Other Stars*, ed. M. Livio
- Jensen, E. L. N., & Mathieu, R. D. 1997, *AJ*, 114, 301
- Jensen, E. L. N., Dhital, S., Stassun, K. G., Patience, J., Herbst, W., Walter, F. M., Simon, M., & Basri, G. 2007, *AJ*, 134, 241
- Kastner, J. H., Huenemoerder, D. P., Schulz, N. S., Canizares, C. R., Li, J., & Weintraub, D. A. 2004, *ApJ*, 605, L49

- Kenyon, S. J., & Hartmann, L. 1987, ApJ, 323, 714
- Koerner, D. W., Ressler, M. E., Werner, M. W., & Backman, D. E. 1998, ApJ, 503, L83
- Koerner, D. et al 2000, ApJ 533, L37.
- Lay, O., Carlstrom, J., and Hills, R. 1997, ApJ 489, 917.
- Lejeune, T. et al 1997, A&AS 125, 229.
- Low, F. J., Smith, P. S., Werner, M., Chen, C., Krause, V., Jura, M., & Hines, D. C. 2005, ApJ, 631, 1170
- Low, F. J., Hines, D. C., & Schneider, G. 1999, ApJ, 520, L45
- Makino, J., 1991, ApJ, 369, 200
- Mamajek, E. E., Meyer, M. R., Hinz, P. M., Hoffmann, W. F., Cohen, M., & Hora, J. L. 2004, ApJ, 612, 496
- Mathieu, R. D., Stassun, K., Basri, G., Jensen, E. L. N., Johns-Krull, C. M., Valenti, J. A., & Hartmann, L. W. 1997, AJ, 113, 1841
- Meyer, M. R., Backman, D. E., Weinberger, A. J., & Wyatt, M. C. 2007, Protostars and Planets V, 573
- Mundy, L. G., Looney, L. W., & Welch, W. J. 2000, Protostars and Planets IV, 355
- Muzerolle, J., Calvet, N., Briceño, C., Hartmann, L., & Hillenbrand, L. 2000, ApJ, 535, L47
- Natta, A., Prusti, T., Neri, R., Wooden, D., Grinin, V. P., & Mannings, V. 2001, A&A, 371, 186
- Natta, A., Testi, L., Calvet, N., Henning, T., Waters, R., & Wilner, D. 2007, Protostars and Planets V, 767
- Perryman, M. A. C., et al. 1997, A&A, 323, L49
- Pichardo, B. et al 2005, MNRAS 359, 521
- Prato, L. et al 2001, ApJ 549, 590 (P2001).
- Soderblom, D. et al 1998, ApJ 498, 385 (S98).
- Sylvester, R. J., Skinner, C. J., Barlow, M. J., & Mannings, V. 1996, MNRAS, 279, 915

- Tokovinin, A. 1999, *Ast. Lett.* 25, 669.
- Torres, G., Stefanik, R. P., Latham, D. W., & Mazeh, T. 1995, *ApJ*, 452, 870
- Trilling, D. E., et al., 2007, *ApJ*, 658, 1289
- Weidenschilling, S. J. 1977, *Ap&SS*, 51, 153
- Weintraub, D. A., Kastner, J. H., & Bary, J. S. 2000, *ApJ*, 541, 767
- Wood, K., Wolff, M. J., Bjorkman, J. E., & Whitney, B. 2002, *ApJ*, 564, 887
- Wyatt, M. C., Smith, R., Greaves, J. S., Beichman, C. A., Bryden, G., & Lisse, C. M. 2006, *ApJ*, 658, 569
- Wyatt, M. C. 2005, *A&A*, 433, 1007
- Wyatt, M. C., Dermott, S. F., Telesco, C. M., Fisher, R. S., Grogan, K., Holmes, E. K., & Pina, R. K. 1999, *ApJ*, 527, 918
- Zuckerman, B., & Becklin, E. E. 1993, *ApJ*, 406, L25